

CGC/saturation approach for soft interactions at high energy: survival probability of the central exclusive production

E. Gotsman,^a E. Levin^{a,b} and U. Maor^a

^a*Department of Particle Physics, School of Physics and Astronomy, Raymond and Beverly Sackler Faculty of Exact Science, Tel Aviv University, Tel Aviv, 69978, Israel*

^b*Departamento de Física, Universidad Técnica Federico Santa María, and Centro Científico-Tecnológico de Valparaíso, Avda. Espana 1680, Casilla 110-V, Valparaíso, Chile*

E-mail: gotsman@post.tau.ac.il, leving@post.tau.ac.il, eugeny.levin@usm.cl, maor@post.tau.ac.il

ABSTRACT: We estimate the value of the survival probability for central exclusive production, in a model, which is based on the CGC/saturation approach. Hard and soft processes are described in the same framework. At LHC energies, we obtain a small value for the survival probability. The source of the small value, is the impact parameter dependence of the hard amplitude. Our model has successfully described a large body of soft data: elastic, inelastic and diffractive cross sections, inclusive production and rapidity correlations, as well as the t -dependence of deep inelastic diffractive production of vector mesons.

KEYWORDS: CGC/saturation approach, survival probability, soft processes

Contents

1	Introduction	1
2	Our model: generalities and the elastic amplitude	3
3	The main formulae for the survival probability	5
3.1	Hard amplitude in the two channel model	5
3.2	Survival probability: eikonal approach	9
3.3	Survival probability: enhanced diagrams	10
3.4	Survival probability: general formulae	11
3.4.1	Survival probability: eikonal formula for two channel model	11
3.4.2	General case: Ω^{hard}	12
3.4.3	Final formula	13
4	Numerical estimates	14
4.1	Survival probability in our model	14
4.2	Importance of b -dependence of the hard amplitude.	15
4.3	Kinematic corrections	17
4.4	Comparison with other estimates	17
5	Conclusions	18
6	Acknowledgements	20

1 Introduction

The large body of experimental data [1–9] on high energy soft interactions from the LHC, calls for an approach based on QCD that allows us to comprehend this data. However, due to the embryonic stage of our understanding of the confinement of quarks and gluons, we are doomed to have to introduce phenomenological model assumptions beyond that of QCD. In our recent articles [10–13] we have proposed an

approach, based on the CGC/saturation effective theory of high energy interactions in QCD (see Refs.[14–20] and Ref.[21] for a review) and the Good-Walker[22] approximation for the structure of hadrons. In the next section we give a brief review of our model, however, we would like to mention here, that the main ingredient of this model, is the BFKL Pomeron[23, 24], which describes both hard and soft processes at high energies. In other words, in our approach, we do not separate the interactions into hard and soft, both are described in the framework of the same scheme. The second important remark concerns the description of the experimental data: we obtain a good description of the cross sections of elastic and diffractive cross sections, of inclusive productions and the rapidity correlations at high energies. Consequently, we feel that we are ready to test our model on a complicated phenomenon, the survival probability of central diffractive production.

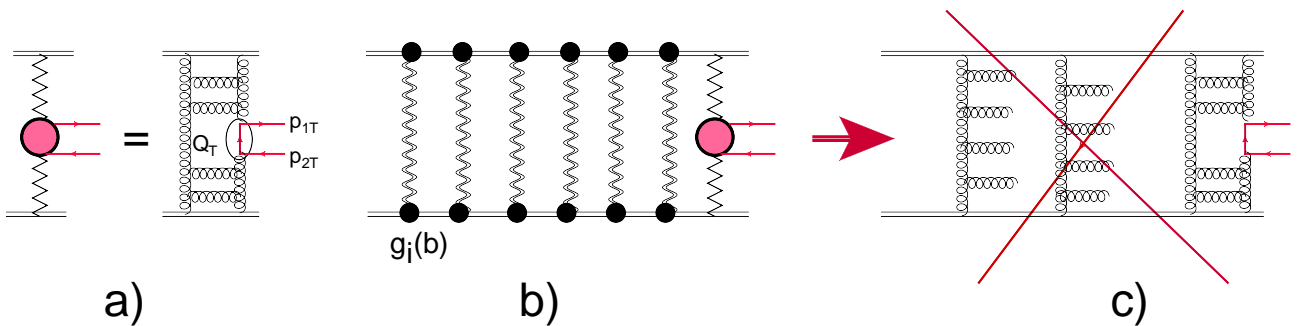


Figure 1. Fig. 1-a shows the scattering amplitude of the hard process. Fig. 1-b describes the set of the eikonal diagrams in the BFKL Pomeron calculus, which suppress the di-jet quark production, due to the contamination of the LRG (large rapidity gap), by gluons that can be produced by different parton showers, as shown in Fig. 1-c.

The physical meaning of "survival probability" has been clarified in the first papers on this subject (see Refs.[25–27]), and is illustrated by Fig. 1, using the example of the central production of a di-jet with large transverse momenta. At first sight we have to calculate the diagram of Fig. 1-a in perturbative QCD, in which only two protons and the di-jet are produced, without any other hadrons. However, this is not sufficient, since simultaneously, a number of parton showers can be produced, and gluons (quarks) from these showers will produce additional hadrons. To calculate central diffractive production, we have to exclude these processes. In other words, we multiply the cross section given by the diagram of Fig. 1-a, by the suppression factor, which reflects the probability of not having any additional parton showers. This factor is the "survival probability".

Even this brief description indicates, that we have a complex problem, since some of the produced parton showers can have perturbative QCD structures, while others can stem from the long distances, and can be non-perturbative by nature. Therefore, to attack this problem we need a model that describes both long and short distances.

As we have mentioned above, our model fulfills these requirements, and so we will proceed to discuss survival probability in this model, expecting reliable results.

The next section is a brief review of our approach. We include it in the paper, for the completeness of presentation, and to emphasize that both short and long distance phenomena are described in the same framework. Section 3 is devoted to derivation of the formulae for the survival probability using the BFKL Pomeron calculus. The numerical estimates are given in section 4, while in the section Conclusions, we summarize our results.

2 Our model: generalities and the elastic amplitude

In this section we briefly review our model which successfully describes diffractive[10, 11] and inclusive cross sections[12]. The main ingredient of our model is the BFKL Pomeron Green function, which we obtained using a CGC/saturation approach[10, 28]. We determined this function from the solution of the non-linear Balitsky-Kovchegov (BK) equation[17, 18], using the MPSI approximation [29] to sum enhanced diagrams, shown in Fig. 2-a. It has the following form:

$$G^{\text{dressed}}(T) = a^2(1 - \exp(-T)) + 2a(1 - a)\frac{T}{1 + T} + (1 - a)^2 G(T) \\ , \quad \text{with} \quad G(T) = 1 - \frac{1}{T} \exp\left(\frac{1}{T}\right) \Gamma_0\left(\frac{1}{T}\right). \quad (2.1)$$

$$T(s, b) = \phi_0 S(b, m) e^{0.63\lambda \ln(s/s_0)}, \quad \text{with} \quad S(b, m) = \frac{m^2}{2\pi} e^{-mb}. \quad (2.2)$$

In the above formulae $a = 0.65$, this value was chosen so as to attain the analytical form of the solution of the BK equation. Parameters λ and ϕ_0 can be estimated in the leading order of QCD, but due to the large next-to-leading order corrections, we consider them as objects to be determined from a fit to the relevant experimental data. m is a non-perturbative parameter, which characterizes the large impact parameter behavior of the saturation momentum, as well, as the typical size of dipoles that take part in the interaction. The value of $m = 5.25 \text{ GeV}$ in our model, supports our main assumption, that the BFKL Pomeron calculus, based on a perturbative QCD approach, is able to describe soft physics, since $m \gg \mu_{\text{soft}}$, where μ_{soft} is the natural scale for soft processes ($\mu_{\text{soft}} \sim \Lambda_{\text{QCD}}$ and/or pion mass).

Unfortunately, in the situation where the confinement problem is still far from being solved, we need to rely on a phenomenological approach for the structure of the colliding hadrons. We use a two channel model, which allows us also to calculate the diffractive production in the region of small masses. In this model, we replace the rich structure of the diffractively produced states, by the single state with the wave function ψ_D . The observed physical hadronic and diffractive states are written in the form

$$\psi_h = \alpha \psi_1 + \beta \psi_2; \quad \psi_D = -\beta \psi_1 + \alpha \psi_2; \quad \text{where} \quad \alpha^2 + \beta^2 = 1; \quad (2.3)$$

Functions ψ_1 and ψ_2 form a complete set of orthogonal functions $\{\psi_i\}$ which diagonalize the interaction matrix \mathbf{T}

$$A_{i,k}^{i'k'} = \langle \psi_i \psi_k | \mathbf{T} | \psi_{i'} \psi_{k'} \rangle = A_{i,k} \delta_{i,i'} \delta_{k,k'}. \quad (2.4)$$

The unitarity constraints take the form

$$2 \operatorname{Im} A_{i,k}(s, b) = |A_{i,k}(s, b)|^2 + G_{i,k}^{in}(s, b), \quad (2.5)$$

where $G_{i,k}^{in}$ denotes the contribution of all non diffractive inelastic processes, i.e. it is the summed probability for these final states to be produced in the scattering of a state i off a state k . In Eq. (2.5) $\sqrt{s} = W$ is the energy of the colliding hadrons, and b denotes the impact parameter. A simple solution to Eq. (2.5) at high energies, has the eikonal form with an arbitrary opacity Ω_{ik} , where the real part of the amplitude is much smaller than the imaginary part.

$$A_{i,k}(s, b) = i(1 - \exp(-\Omega_{i,k}(s, b))), \quad (2.6)$$

$$G_{i,k}^{in}(s, b) = 1 - \exp(-2\Omega_{i,k}(s, b)). \quad (2.7)$$

Eq. (2.7) implies that $P_{i,k}^S = \exp(-2\Omega_{i,k}(s, b))$ is the probability that the initial projectiles (i, k) will reach the final state interaction unchanged, regardless of the initial state re-scatterings.

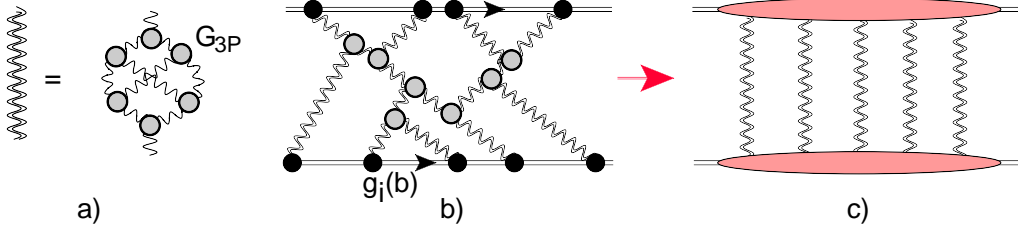


Figure 2. Fig. 2-a shows the set of the diagrams in the BFKL Pomeron calculus that produce the resulting (dressed) Green function of the Pomeron in the framework of high energy QCD. In Fig. 2-b the net diagrams which include the interaction of the BFKL Pomerons with colliding hadrons are shown. After integration over positions of G_{3P} in rapidity, the sum of the diagrams reduces to Fig. 2-c .

Note, that there is no factor $1/2$. Its absence stems from our definition of the dressed Pomeron.

2 ch. model	λ	$\phi_0 (GeV^{-2})$	$g_1 (GeV^{-1})$	$g_2 (GeV^{-1})$	$m(GeV)$	$m_1(GeV)$	$m_2(GeV)$	β
old set	0.38	0.0019	110.2	11.2	5.25	0.92	1.9	0.58
new set	0.325	0.0021	118	14.7	5.45	1.04	0.47	0.52

Table 1. Fitted parameters of the model. The values of the old set are taken from Ref.[11]. Values of the new set are determined by fitting to data with the additional constraint $m_2 \leq 1.5$ GeV. See Section 4.2.

In the eikonal approximation we replace $\Omega_{i,k}(s, b)$ by

$$\Omega_{i,k}(s, b) = \int d^2b' d^2b'' g_i(\vec{b}') G^{\text{dressed}}(T(s, \vec{b}'')) g_k(\vec{b} - \vec{b}' - \vec{b}''). \quad (2.8)$$

We propose a more general approach, which takes into account new small parameters that result from the fit to the experimental data (see Table 1 and Fig. 2):

$$G_{3P}/g_i(b=0) \ll 1; \quad m \gg m_1 \text{ and } m_2. \quad (2.9)$$

The second equation in Eq. (2.9) means that b'' in Eq. (2.8) is much smaller than b and b' , therefore, Eq. (2.8) can be re-written in a simpler form

$$\begin{aligned}\Omega_{i,k}(s,b) &= \left(\int d^2 b'' G^{\text{dressed}} \left(T(s, \vec{b}'') \right) \right) \int d^2 b' g_i(\vec{b}') g_k(\vec{b} - \vec{b}') \\ &= \tilde{G}^{\text{dressed}}(\bar{T}) \int d^2 b' g_i(\vec{b}') g_k(\vec{b} - \vec{b}').\end{aligned}\quad (2.10)$$

Selecting the diagrams using the first equation in Eq. (2.9), one can see, that the main contribution stems from the net diagrams shown in Fig. 2-b. The sum of these diagrams[11] leads to the following expression for $\Omega_{i,k}(s,b)$

$$\Omega(Y;b) = \int d^2 b' \frac{g_i(\vec{b}') g_k(\vec{b} - \vec{b}') \tilde{G}^{\text{dressed}}(\bar{T})}{1 + G_{3P} \tilde{G}^{\text{dressed}}(\bar{T}) [g_i(\vec{b}') + g_k(\vec{b} - \vec{b}')]}; \quad (2.11)$$

$$g_i(b) = g_i S_p(b; m_i); \quad (2.12)$$

where

$$\begin{aligned}S_p(b, m_i) &= \frac{1}{4\pi} m_i^3 b K_1(m_i b), \\ \tilde{G}^{\text{dressed}}(\bar{T}) &= \int d^2 b G^{\text{dressed}}(T(s, b)),\end{aligned}$$

where $T(s, b)$ is given by Eq. (2.2).

Note that $\tilde{G}^{\text{dressed}}(\bar{T})$ does not depend on b , and is a function of $\bar{T} = T(s, b=0) = \phi_0 e^{0.63 \lambda Y}$.

In the above formulae the value of the triple BFKL Pomeron vertex is known: $G_{3P} = 1.29 \text{ GeV}^{-1}$.

For further discussion we introduce

$$N^{BK}(G_{\mathcal{P}}^i(Y, b)) = a (1 - \exp(-G_{\mathcal{P}}^i(Y, b))) + (1 - a) \frac{G_{\mathcal{P}}^i(Y, b)}{1 + G_{\mathcal{P}}^i(Y, b)}, \quad (2.13)$$

with $a = 0.65$. Eq. (2.13) is the analytical approximation for the numerical solution to the BK equation[28]. $G_{\mathcal{P}}(Y; b) = g_i(b) \tilde{G}^{\text{dressed}}(\bar{T})$. We recall that the BK equation sums the ‘fan’ diagrams shown in Fig. 3.

3 The main formulae for the survival probability

3.1 Hard amplitude in the two channel model

The expression for the hard amplitude is known, and it has been discussed in great detail (see Ref.[30]). It has the following general form (see Fig. 1-a)

$$A^{\text{hard}} = \pi^2 \int d^2 Q_T \frac{\bar{M}}{Q_T^2 (\vec{Q}_T - \vec{p}_{1T})^2 (\vec{Q}_T + \vec{p}_{2T})^2} \phi_G(x_1, x'_1, Q_T^2, t_1) \phi_G(x_2, x'_2, Q_T^2, t_2). \quad (3.1)$$

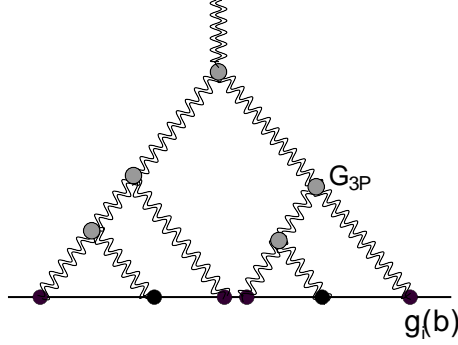


Figure 3. A typical example of ‘fan’ diagrams that are summed in Eq. (2.13).

where Q_T is the transverse momentum in the gluon loop, $\bar{\mathcal{M}}$ is the color averaged amplitude for the process $GG \rightarrow X$, where X denotes the final state (quark-antiquark jets in Fig. 1-a) with mass M_X .

$$\bar{\mathcal{M}} = \frac{2}{M_X^2} \frac{1}{N_c^2 - 1} \sum_{a,b} \delta^{ab} \left(\vec{Q}_T^\mu - \vec{p}_{1T}^\mu \right) \left(\vec{Q}_T^\nu + \vec{p}_{2T}^\nu \right) \Gamma_{\mu\nu}^{ab}. \quad (3.2)$$

$\Gamma_{\mu\nu}^{ab}$ is a vertex for $GG \rightarrow X$.

$\phi_G(x_i, x'_i, Q_T^2, t_i)$ denotes the skewed unintegrated gluon densities. These functions have been discussed and we refer the reader to Ref.[30]. The t_i dependence, is of great importance for the calculation of the survival probability [27, 31]. We show below that the essential t_i turns out to be small in our estimates, and therefore, we have to rely on some input from non-perturbative QCD. Our assumption is that at small t_i we can factorize the unintegrated gluon density as

$$\phi_G(x_i, x'_i, Q_T^2, t_i) = \tilde{\phi}_G(x_i, x'_i, Q_T^2) \Gamma(t_i) \xrightarrow{\text{impact parameter image}} \tilde{\phi}_G(x_i, x'_i, Q_T^2) S^h(b). \quad (3.3)$$

Making the assumption, the hard amplitude at fixed impact parameter b , has the form

$$A^{\text{hard}} = A^{\text{hard}}(s; b, p_1, p_2) \int d^2b' S^h(b') S^h(\vec{b} - \vec{b}'). \quad (3.4)$$

The advantage of our technique is that it is based on the CGC/saturation approach, and the unintegrated structure functions $\phi_G(x_i, x'_i, Q_T^2, t_i)$, can be calculated in this framework. In the two channel model we have two unintegrated structure functions (see Fig. 4):

$$\begin{aligned} \phi_{1 \rightarrow \text{proton}} &\propto \alpha g_1(b) \equiv S_1^h(b); \\ \phi_{2 \rightarrow \text{proton}} &\propto \beta g_2(b) \equiv S_2^h(b); \end{aligned}$$

We extract the b dependence of hard amplitudes i , from the experimental data for diffractive production of vector mesons in deep inelastic scattering (DIS). Presenting the t -dependance of the measure differential

cross section in the form

$$\frac{d\sigma(\gamma^* + p \rightarrow V + p)}{dt} \bigg/ \frac{d\sigma(\gamma^* + p \rightarrow V + p)}{dt} \bigg|_{t=0} = e^{-B^h |t|}. \quad (3.5)$$

In QCD

$$\begin{aligned} \frac{d\sigma(\gamma^* + p \rightarrow V + p)}{dt} &\propto \phi_G^2(x_{Bj}, x'_{Bj}, Q^2, t) \\ &\propto \left(\int e^{i\vec{Q}_T \cdot \vec{b}} (\alpha^2 g_1 S_p(b, m_1) + \beta^2 g_2 S_p(b, m_2)) \right)^2, \end{aligned} \quad (3.6)$$

where $t = -Q_T^2$.

The value of the slope B^h can be calculated and it is equal to

$$B^h = \frac{1}{2} \frac{\int b^2 d^2b (\alpha^2 g_1 S_p(b, m_1) + \beta^2 g_2 S_p(b, m_2))}{\int d^2b (\alpha^2 g_1 S_p(b, m_1) + \beta^2 g_2 S_p(b, m_2))}. \quad (3.7)$$

Using the parameters of Table 1, we find $B^h \approx 4.5 \text{ GeV}^{-2}$. From Fig. 5 one can see that $B^h \rightarrow 4 \div 5 \text{ GeV}^{-2}$. Therefore, the b dependence obtained from our approach, is in accord with the HERA experimental data.

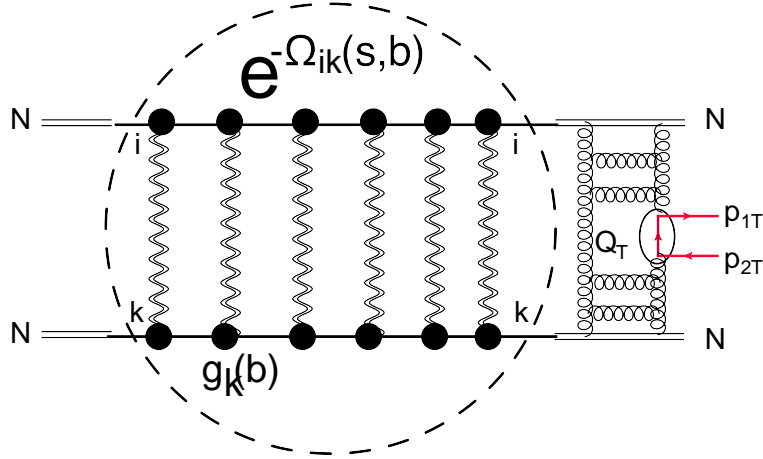


Figure 4. Survival probability in two channel model.

Generally speaking, both B^h 's depend on energy. Indeed, in Regge theory [32], the scattering amplitude $A^{\text{hard}} \propto s^{\alpha_P(t)}$ with $\alpha_P(t) = \alpha_P(0) + \alpha'_P \ln(s/s_0)$ $t = 1 + \Delta + \alpha'_P \ln(s/s_0)$. For hard processes we do not expect Pomeron trajectories with $\alpha'_P \neq 0$. However, the effective α'_P is due to shadowing corrections. The hard amplitude has the following generic form

$$A^{\text{hard}} \propto s^\Delta e^{-\frac{b^2}{2B^h}}. \quad (3.8)$$

At large b this amplitude is small. At some value of $b = b_0(s)$, $A^{\text{hard}}(s, b) \sim 1$. This equation leads to

$$e^{-\frac{b_0^2}{2B^h}} = f \leq 1; \quad b_0^2(s) = 2B^h \Delta \ln(s/s_0). \quad (3.9)$$

Due to unitarity (see Eq. (2.5)) the amplitude cannot exceed unity. Therefore, at $b \leq b_0(s)$, $A^{\text{hard}}(s, b) \propto \Theta(b_0(s) - b)$ where $\Theta(z)$ is a step function. On the other hand, the t slope of the amplitude, is equal to $B = 4\langle b^2 \rangle = 8b_0^2(s)$. The last equation stems from $A^{\text{hard}}(s, b) \propto \Theta(b_0(s) - b)$. Finally, the t -slope for the scattering amplitude is proportional to $\ln(s/s_0)$, viz. $B = \frac{1}{4} B^h \Delta \ln(s/s_0)$ or

$$\alpha_{\mathbb{P}}'^{\text{eff}} = \frac{1}{4} \Delta B_{el,0}^h, \quad (3.10)$$

where B_0^h is the slope for the cross section at $s = s_0$. Choosing $s_0 = 1 \text{ GeV}^2$ and $\Delta = 0.2^*$ we obtain $B_0^h \approx 3.2 \text{ GeV}^{-2}$ and $\alpha_{\mathbb{P}}'^{\text{eff}} = 0.154 \text{ GeV}^{-2}$. While the HERA experiment gives [33, 34] $B_{el}^h = 4.6 \pm 0.06 + 4 (0.164 \pm 0.41) \ln(W/W_0)$. We believe that our approach provides a reasonable estimate of, and an appropriate method to understand the energy behavior of the hard amplitude. Note, that $B_0^h \approx 3.2 \text{ GeV}^{-2}$ comes from the experimental formulae changing $W_0 = 90 \text{ GeV}$ to $W_0 = 1 \text{ GeV}$.

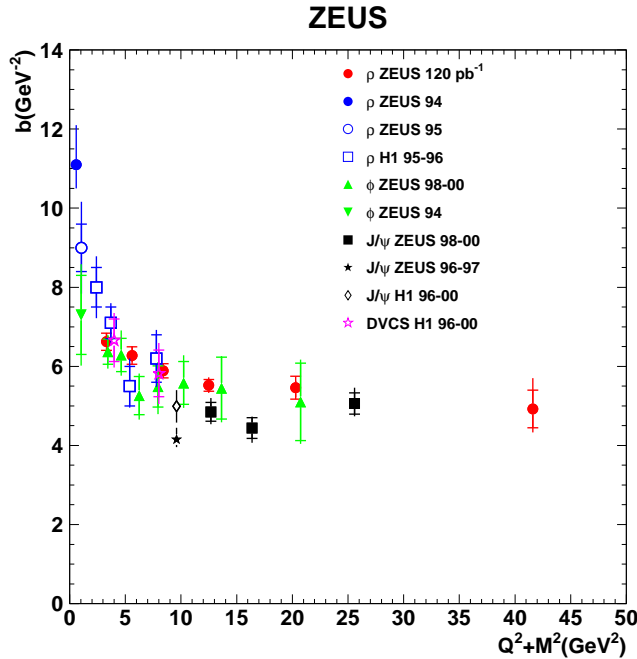


Figure 5. Compilation of experimental data on the slope of the diffractively produced vector mesons at HERA. The figure is taken from Ref.[33]

Bearing in mind this estimate, we find the following hierarchy of transverse distances, in our approach for high energy scattering (see Table 1)

$$\frac{4}{m_1^2} > B^{\text{hard}} \gg \frac{1}{m^2}, \quad (3.11)$$

where $4/m_i^2$ is the typical slope for $g_i(b)$.

* Such values of Δ come both from experiment [33, 34] and from theoretical estimates.

3.2 Survival probability: eikonal approach

Central exclusive production (CEP) has the typical form

$$p + p \rightarrow p(q_{1,T}) + [LRG] + X(M_X) + [LRG] + p(q_{2,T}), \quad (3.12)$$

where LRG denotes the large rapidity gap in which no hadrons are produced. We cannot restrict ourselves to the hard amplitude (see Fig. 1-a) to describe this reaction. Indeed, Eq. (3.1) gives the amplitude of CEP, but only for one parton shower. However, the production of many parton showers, shown in Fig. 1-c, will contaminate the LRG's, and these have to be eliminated, in order to obtain the correct cross section for the reaction of Eq. (3.12). In simple eikonal models, such a suppression stems from the diagrams shown in Fig. 1-b.

For this simple case, we can derive the formula for the survival probability, using two different approaches. The first one, relies on the s-channel unitarity constraint (see Eq. (2.5)). In the eikonal approach the contribution of all inelastic states is given by Eq. (2.7)

$$G_{in}(s, b) = 1 - \exp(-2\Omega(s, b)). \quad (3.13)$$

From Eq. (3.13) we see that multiplying the hard cross section by the factor $\exp(-2\Omega(s, b))$, we obtain the probability that the process has no inelastic production in the entire kinematic rapidity region [25–27]. Therefore, the survival probability factor $\langle S^2 \rangle$ takes the form

$$\begin{aligned} \langle S^2 \rangle &= \frac{\int d^2b e^{-2\Omega(s, b)} \left| A^{\text{hard}}(s; b, p_1, p_2) \int d^2b' S_h(b') S_h(\vec{b} - \vec{b}') \right|^2}{\int d^2b \left| \int d^2b' A^{\text{hard}}(s; b, p_1, p_2) S_h(b') S_h(\vec{b} - \vec{b}') \right|^2} \\ &= \frac{\int d^2b e^{-2\Omega(s, b)} \left| \int d^2b' S_h(b') S_h(\vec{b} - \vec{b}') \right|^2}{\int d^2b \left| \int d^2b' S_h(b') S_h(\vec{b} - \vec{b}') \right|^2}. \end{aligned} \quad (3.14)$$

The second derivation is based on summing the Pomeron diagrams of Fig. 1-b, introducing $\Omega = g(b)^2 \tilde{G}^{\text{dressed}}(s)$ in Eq. (3.13). The eikonal amplitude can be written as (see Eq. (2.6))

$$i(1 - \exp(-\Omega(s, b))) = i \sum_{n=1}^{\infty} (-1)^{n-1} \frac{\Omega^n(s, b)}{n!}. \quad (3.15)$$

In each term with the exchange of n -Pomerons, we need to replace one of these Pomerons by the hard amplitude. Such a replacement leads to the following sum

$$i \sum_{n=1}^{\infty} (-1)^{n-1} \frac{n \Omega^n(s, b)}{n!} A^{\text{hard}} = i e^{-\Omega(s, b)} A^{\text{hard}}. \quad (3.16)$$

Multiplying this amplitude by its complex conjugate, and integrating over b we obtain Eq. (3.14).

3.3 Survival probability: enhanced diagrams

At first sight Eq. (3.14), provides the answer for the case of eikonal rescattering. However, this is not correct, since the dressed BFKL Pomeron Green function is the sum of enhanced diagrams of Fig. 2-a and Fig. 6-a. To find the survival probability, we need to replace one of the Pomeron lines in Fig. 6-a by the hard amplitude. As was noticed in Ref.[35] the enhanced diagrams can be reduced to a sum of diagrams which have a general form

$$G^{\text{dressed}}(T) = \sum_{n=1}^{\infty} (-1)^{n-1} \Gamma^2(P \rightarrow nP) T^n, \quad (3.17)$$

after integration over positions in rapidity, of the triple Pomeron vertices. The vertices $\Gamma(P \rightarrow nP)$ can easily be found from Eq. (2.1). To obtain the survival probability, we need to replace T in Eq. (3.17) by the hard amplitude : viz

$$\begin{aligned} G^{\text{hard}}(Y, b) &\equiv A_{\mathbb{P}}^{\text{hard}} \sum_{n=1}^{\infty} (-1)^n n \Gamma^2(P \rightarrow nP) T^{n-1} \\ &\rightarrow A_{\mathbb{P}}^{\text{hard}} \left\{ a^2 e^{-T} - (1-a) \left(\frac{1-a}{T^2} - \frac{2a}{(1+T)^2} \right) + (1-a)^2 \frac{1+T}{T^3} e^{\frac{1}{T}} \Gamma_0 \left(\frac{1}{T} \right) \right\}. \end{aligned} \quad (3.18)$$

It should be noted that $A_{\mathbb{P}}^{\text{hard}}$ is not the same as in Eq. (3.14), and its b distribution has a typical value of $b \propto 1/m$. In other words $A_{\mathbb{P}}^{\text{hard}} \propto S(b)$. Eq. (3.18) leads to the following contribution

$$\Omega_{ik}^{\text{hard}} = \int d^2 b' d^2 b'' g_i(b') G^{\text{hard}}(Y, b'') g_k(\vec{b} - \vec{b}' - \vec{b}'') \rightarrow \int d^2 b' g_i(b') g_k(\vec{b} - \vec{b}') \tilde{G}^{\text{hard}}(Y) \quad (3.19)$$

$$\tilde{G}^{\text{hard}}(Y) = \int d^2 b'' S(b'') \left\{ a^2 e^{-T} - (1-a) \left(\frac{1-a}{T^2} - \frac{2a}{(1+T)^2} \right) + (1-a)^2 \frac{1+T}{T^3} e^{\frac{1}{T}} \Gamma_0 \left(\frac{1}{T} \right) \right\}. \quad (3.20)$$

Inspecting Eq. (3.19) we note that at $T \rightarrow 0$, Eq. (3.19) leads to $\Omega_{ik}^{\text{hard}} \rightarrow \int d^2 b' d^2 b'' g_i(b') g_k(\vec{b} - \vec{b}') \tilde{G}^{\text{hard}}(Y)$, which coincides with our hard amplitude introduced in Eq. (3.5). Using the notation in this equation, the expression for $\Omega_{ik}^{\text{hard}}$ takes the final form:

$$\Omega_{ik}^{\text{hard}} = \int d^2 b' S_i^h(b') S_k^h(\vec{b} - \vec{b}') \tilde{G}^{\text{hard}}(Y). \quad (3.21)$$

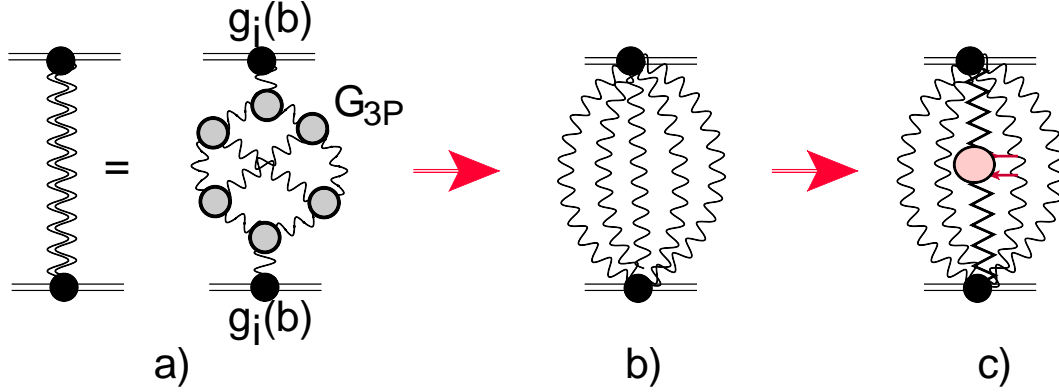


Figure 6. Fig. 6-a shows the set of the diagrams for the BFKL Pomeron calculus that lead to the resulting Pomeron Green function, after integrating over rapidities of the triple Pomeron vertices, can be re-written in the form of Fig. 6-b. Fig. 6-c illustrates that to calculate the survival probability, we need to replace one of BFKL Pomerons by the hard amplitude.

3.4 Survival probability: general formulae

3.4.1 Survival probability: eikonal formula for two channel model

The structure of the formula for the survival probability is shown in Fig. 4. The amplitude for the reaction of Eq. (3.12) can be written in the form

$$\begin{aligned}
A^{full}(s, q_{1,T}, q_{2,T}, p_1, p_1) &= \int d^2b' d^2b e^{i\vec{q}_{1,T} \cdot \vec{b}'} e^{i\vec{q}_{2,T} \cdot (\vec{b} - \vec{b}')} \tilde{G}^{hard}(Y) \\
&\times \left\{ \alpha^2 e^{-\Omega_{11}(s,b)} S_1^h(b') S_1^h(\vec{b} - \vec{b}') + \beta^2 e^{-\Omega_{22}(s,b)} S_2^h(b') S_2^h(\vec{b} - \vec{b}') \right. \\
&\left. + \alpha \beta \left(e^{-\Omega_{12}(s,b)} S_1^h(b') S_2^h(\vec{b} - \vec{b}') + e^{-\Omega_{21}(s,b)} S_2^h(b') S_1^h(\vec{b} - \vec{b}') \right) \right\}. \quad (3.22)
\end{aligned}$$

The survival probability for the cross section $d^2\sigma/(dt_1 dt_2)$ is equal

$$\langle S^2 \rangle = \left| A^{full}(s, q_{1,T}, q_{2,T}, p_1, p_1) \right|^2 / \left| A^{hard}(s, q_{1,T}, q_{2,T}, p_1, p_1) \right|^2, \quad (3.23)$$

where

$$\begin{aligned}
A^{hard}(s, q_{1,T}, q_{2,T}, p_1, p_1) &= \int d^2b' d^2b e^{i\vec{q}_{1,T} \cdot \vec{b}'} e^{i\vec{q}_{2,T} \cdot (\vec{b} - \vec{b}')} \\
&\times \left\{ \alpha^2 S_1^h(b') S_1^h(\vec{b} - \vec{b}') + \beta^2 S_2^h(b') S_2^h(\vec{b} - \vec{b}') + \alpha \beta \left(S_1^h(b') S_2^h(\vec{b} - \vec{b}') + S_2^h(b') S_1^h(\vec{b} - \vec{b}') \right) \right\}. \quad (3.24)
\end{aligned}$$

However, if we are interested in cross sections that are integrated over $d^2q_{1,T}$ and $d^2q_{2,T}$, the expression for $\langle S^2 \rangle$ can be simplified, and it has the form

$$\langle S^2 \rangle = N(s, M_x, p_1, p_2) / D(s, M_x, p_1, p_2), \quad (3.25)$$

with

$$\begin{aligned} N(s, M_x, p_1, p_2) &= \int d^2 b \left(\tilde{G}^{\text{hard}}(Y) \right)^2 \\ &\times \left\{ \int d^2 b' \left(\alpha^2 e^{-\Omega_{11}(s, b)} S_1^h(b') S_1^h(\vec{b} - \vec{b}') + \beta^2 e^{-\Omega_{22}(s, b)} S_2^h(b') S_2^h(\vec{b} - \vec{b}') \right. \right. \\ &\left. \left. + \alpha \beta \left(e^{-\Omega_{12}(s, b)} S_1^h(b') S_2^h(\vec{b} - \vec{b}') + e^{-\Omega_{21}(s, b)} S_2^h(b') S_1^h(\vec{b} - \vec{b}') \right) \right) \right\}^2, \end{aligned} \quad (3.26)$$

and

$$\begin{aligned} D(s, M_x, p_1, p_2) &= \int d^2 b \left\{ \int d^2 b' \left(\alpha^2 S_1^h(b') S_1^h(\vec{b} - \vec{b}') + \beta^2 S_2^h(b') S_2^h(\vec{b} - \vec{b}') \right. \right. \\ &\left. \left. + \alpha \beta \left(S_1^h(b') S_2^h(\vec{b} - \vec{b}') + S_2^h(b') S_1^h(\vec{b} - \vec{b}') \right) \right) \right\}^2. \end{aligned} \quad (3.27)$$

3.4.2 General case: Ω^{hard}

The first problem that we need to solve, is to find a more general expression for Ω^{hard} , than we have obtained in Eq. (3.21). Eq. (2.11) sums net diagrams, and they can be re-written in the same form as the enhanced ones[35]. Eq. (3.17) is replaced by

$$\Omega_{ik} = \sum_{n=1}^{\infty} (-1)^{n-1} \Gamma(i \rightarrow nP) \Gamma(k \rightarrow nP) \left(\tilde{G}^{\text{dressed}} \right)^n. \quad (3.28)$$

From Eq. (3.28) we obtain

$$\Omega_{ik}^{\text{hard}} = A^{\text{hard}} \sum_{n=0}^{\infty} \Gamma(i \rightarrow (n+1)P) \Gamma(k \rightarrow (n+1)P) \left(\tilde{G}^{\text{dressed}} \right)^n. \quad (3.29)$$

Using Eq. (2.11) and Eq. (3.29) we obtain

$$\Omega_{ik}^{\text{hard}}(Y; b) = \int d^2 b' \frac{S_h^i(\vec{b}') S_h^k(\vec{b} - \vec{b}')}{\left(1 + G_{3P} \tilde{G}^{\text{dressed}}(T) \left[g_i(\vec{b}') + g_k(\vec{b} - \vec{b}') \right] \right)^2}. \quad (3.30)$$

Taking into account the enhanced diagrams for $\tilde{G}^{\text{dressed}}$ (see Eq. (3.19)) we obtain the final form for $\Omega_{ik}^{\text{hard}}$:

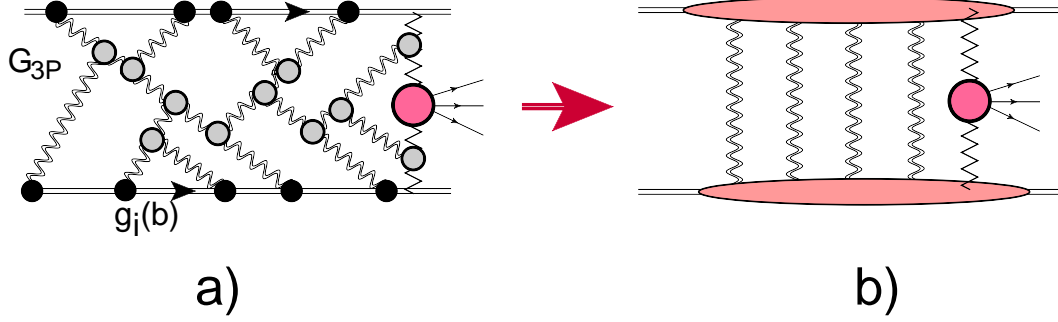


Figure 7. Fig. 7-a shows the set of the net diagrams in the BFKL Pomeron calculus, that lead to the resulting survival probability in the framework of high energy QCD. After integration over positions of G_{3P} in rapidity, the sum of the diagrams reduces to Fig. 7-b.

$$\Omega_{ik}^{\text{hard}}(Y; b) = \int d^2b' \tilde{G}^{\text{hard}}(Y) \frac{S_h^i(\vec{b}') S_h^k(\vec{b} - \vec{b}')}{\left(1 + G_{3P} \tilde{G}^{\text{dressed}}(T) [g_i(\vec{b}') + g_k(\vec{b} - \vec{b}')] \right)^2} = \tilde{G}^{\text{hard}}(Y) \bar{\Omega}_{ik}^{\text{hard}}. \quad (3.31)$$

3.4.3 Final formula

Finally, to obtain the general formula for the survival probability we need in Eq. (3.26), we replace $\int d^2b' S_h^i(\vec{b}') S_h^k(\vec{b} - \vec{b}')$ by $\bar{\Omega}_{ik}^{\text{hard}}(Y, b)$. Therefore, the survival probability is equal to

$$\langle S^2 \rangle = N(s, M_x, p_1, p_2) / D(s, M_x, p_1, p_2), \quad (3.32)$$

with

$$\begin{aligned} N(s, M_x, p_1, p_2) = & \int d^2b \left(\tilde{G}^{\text{hard}}(Y) \right)^2 \times \left\{ \alpha^2 e^{-\Omega_{11}(s, b)} \bar{\Omega}_{11}^{\text{hard}}(Y, b) + \beta^2 e^{-\Omega_{22}(s, b)} \bar{\Omega}_{22}^{\text{hard}}(Y, b) \right. \\ & \left. + \alpha \beta \left(e^{-\Omega_{12}(s, b)} \bar{\Omega}_{12}^{\text{hard}}(Y, b) + e^{-\Omega_{21}(s, b)} \bar{\Omega}_{21}^{\text{hard}}(Y, b) \right) \right\}^2. \end{aligned} \quad (3.33)$$

while $D(s, M_x, p_1, p_2)$ remains the same as in Eq. (3.27).

From Eq. (3.32) and Eq. (3.33) we note that $\langle S^2 \rangle \propto \left(\tilde{G}^{\text{hard}}(Y) \right)^2$. This factor takes into account the contribution from the enhanced diagrams. Fig. 8 shows that on its own, it leads to a smaller survival probability.

4 Numerical estimates

4.1 Survival probability in our model

Our estimates for the survival probability are shown in Fig. 9.

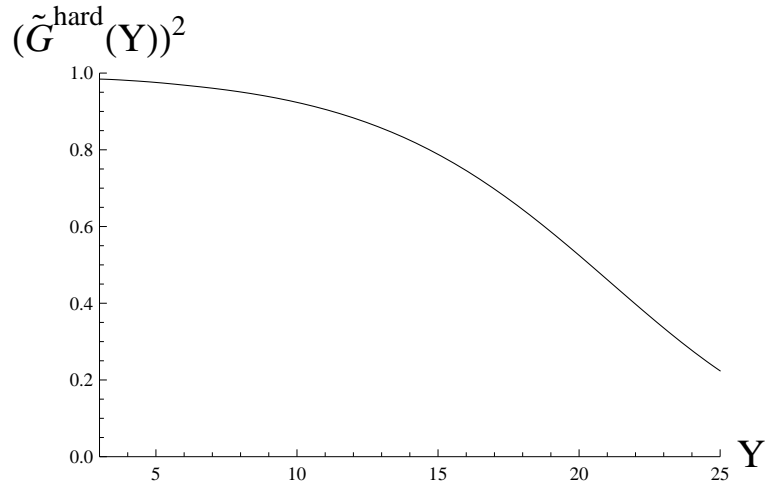


Figure 8. The suppression factor $\left(\tilde{G}^{\text{hard}}(Y)\right)^2$ which includes the contribution of the enhanced diagrams.

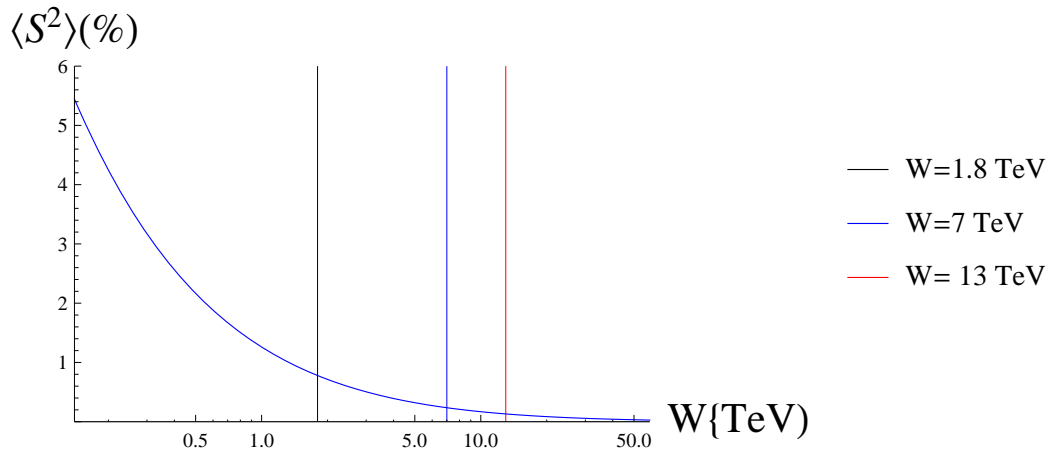


Figure 9. $\langle S^2 \rangle$ of Eq. (3.32) versus W .

We predict rather small values for the survival probability. Such small values have been discussed previously (see Ref.[31]), however, in the present model we have a different source for this small number. In Ref.[31] $\langle S^2 \rangle$ turns out to be small, due to contribution of the enhanced diagram, while in the present model the enhanced diagrams give a suppression factor which is moderate (see Fig. 8). The main cause for the small value of $\langle S^2 \rangle$, is the b dependence of the hard amplitude. As we have mentioned our b dependence

stems from the description of the soft high energy data, based on CGC/saturation approach, in which we do not introduce a special soft amplitude. In our approach we are only dealing with hard (semi-hard) amplitudes, which provide a smooth matching of the ‘soft’ interaction with the ‘hard’ one.

4.2 Importance of b -dependence of the hard amplitude.

We can illustrate the importance of the b -dependence of the hard amplitude by introducing

$$\begin{aligned} S_1^h &= \alpha \frac{1}{2\pi B^h} e^{-\frac{b^2}{2B^h}}; \\ S_2^h &= \beta \frac{1}{2\pi B^h} e^{-\frac{b^2}{2B^h}}; \end{aligned} \quad (4.1)$$

with $B^h = 4 \div 5 \text{ GeV}^{-2}$, which follows from the experimental data, as discussed previously. At first sight Eq. (4.1) follows from the experimental observation of the vector meson production in deep inelastic scattering. As we have discussed, our hard amplitude of Eq. (3.5) leads to the slope of the differential cross section which is the same as in Eq. (4.1). Indeed, as shown in Fig. 10, the t -dependence of the differential cross sections in the region of small t ($t < 0.5 \text{ GeV}^2$), are similar in both parametrizations of the hard amplitude. However, at large t there is a difference, which increases with increasing t .

The difference between the amplitudes is more pronounced when plotted as a function of the impact parameter b (see Fig. 11).

Figure Fig. 11 shows that Eq. (3.5) of our model (with the old set of parameters) leads to fast decrease of the amplitude in b . As one can see from Table 1, the steepest decrease is due to the $A_{22}(b)$ amplitude, which is the smallest. This amplitude also has the smallest suppression, due to the factors $\exp(-2\Omega_{ik})$, since Ω_{22} has the smallest value. In the numerator of Eq. (3.32), only term (22) provides the essential contribution. This term turns out to be rather large for the amplitude of Eq. (4.1), as one can see from Fig. 11. On the other hand, the same hard amplitude in Eq. (3.5) shows the steep decrease in b , resulting in the small contribution to the numerator of Eq. (3.32), as well as for the resulting $\langle S^2 \rangle$.

The resulting difference for $\langle S^2 \rangle$ is large, values of the survival probability for the hard amplitude of Eq. (4.1), are ten or more, times larger than the results of our present model (with the old set of parameters). For example, for $W = 7 \text{ TeV}$ we obtain $\langle S^2 \rangle = 10 \div 15\%$.

We denote our fit which results in these very low values of $\langle S^2 \rangle$ as the "old set of parameters". Based on the our diagnosis of the problem above, we made a second fit to the same experimental data, with the additional condition that $m_2 \leq 1.5 \text{ GeV}$. We will refer to this fit as "new set of parameters". The values of the parameters for both "old" and "new" sets are given in Table 1. The comparison of the results for $\sigma_{tot}, \sigma_{el}, B_{el}, \sigma_{sd}$ (low and high mass) and σ_{dd} (low and high mass) for both set of parameters are shown in Table 4. We note that the values of $\sigma_{tot}, \sigma_{el}$ and B_{el} obtained in both fits are rather close, while the diffractive cross sections, both σ_{sd} and σ_{dd} are smaller in the new fit.

The results for $\langle S^2 \rangle$ for the "new set of parameters" is shown in Fig.12, we find $\langle S^2 \rangle \approx 3 \%$ in the LHC energy range.

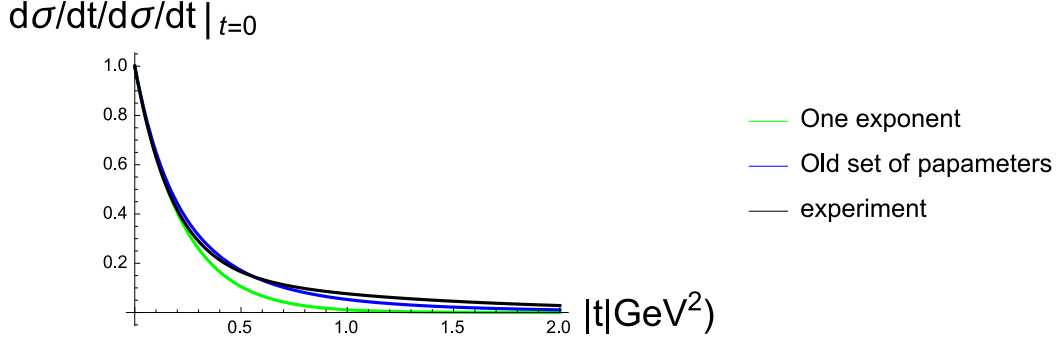


Fig. 10-a

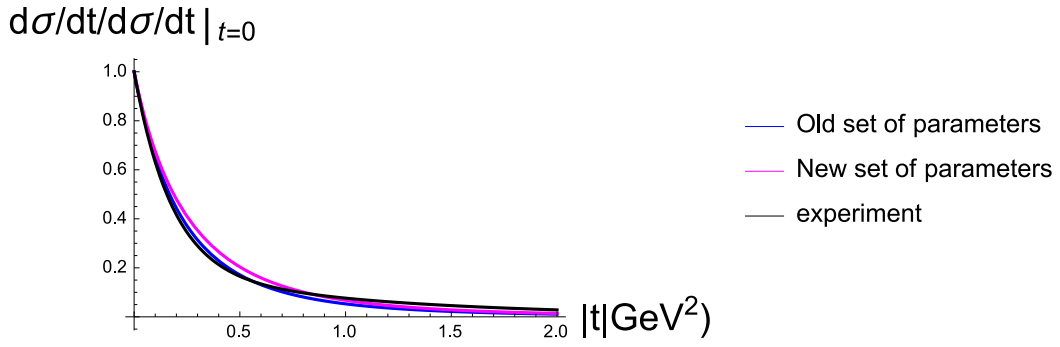


Fig. 10-b

Figure 10. $d\sigma/dt / (d\sigma/dt|_{t=0})$ versus $|t|$: in Fig. 10-a for Eq. (3.5) (blue, ‘one exponents’ curve), Eq. (3.6) for hard amplitude in our model, and black curve which is the fit to the experimental data taken from Ref. [36]; and in Fig. 10-b blue curve corresponds to the old set of the parameters in our model while the red line describes the prediction of our model with the new set of the parameters. The typical experimental errors are ± 0.025 .

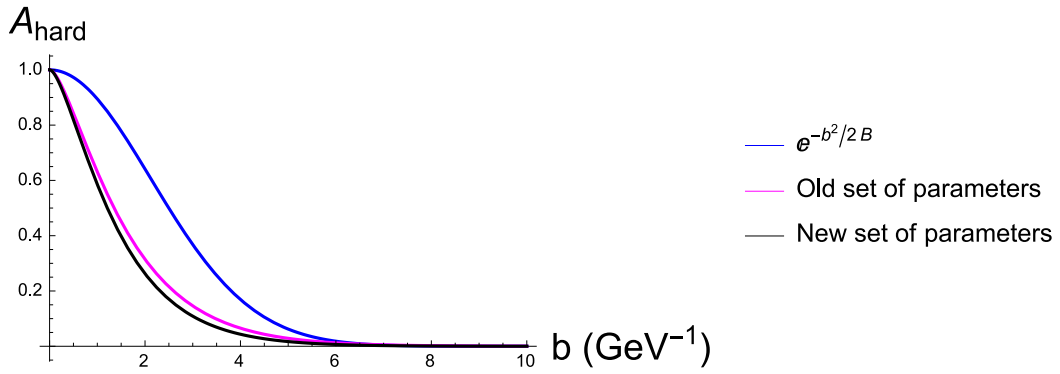


Figure 11. Comparison of hard amplitudes defined in Eq. (3.5) and Eq. (4.1).

4.3 Kinematic corrections

In our approach we consider G_{3P} as a point-like vertex. This assumption is a considerable simplification. As we have discussed in [13], we expect short range correlations in rapidity, with the correlation length in rapidity $\Delta_{cor} \approx 2$. Bearing in mind that the triple Pomeron vertex has a size in rapidity, we can take into consideration that in Eq. (3.17) and Eq. (3.28), the Pomerons enter not at rapidity Y but at $Y - \delta_{cor} N_{G_{3P}}$, where $N_{G_{3P}}$ is the average number of triple Pomeron vertices. It is easy to see that

$$N_{G_{3P}} = \int d^2b T(Y, b) \frac{dG^{\text{dressed}}(T(Y, b))}{T(Y, b)} \bigg/ \int d^2b G^{\text{dressed}}(T(Y, b)). \quad (4.2)$$

In Fig. 12 we plot $\langle S^2 \rangle$ which is given by Eq. (3.32) and Eq. (3.33) but $Y \rightarrow Y - \Delta_{cor} N_{G_{3P}}$ with $N_{G_{3P}}$ estimated using Eq. (4.2). One can see that the effect is sizeable, and leads to larger values of the survival probability.

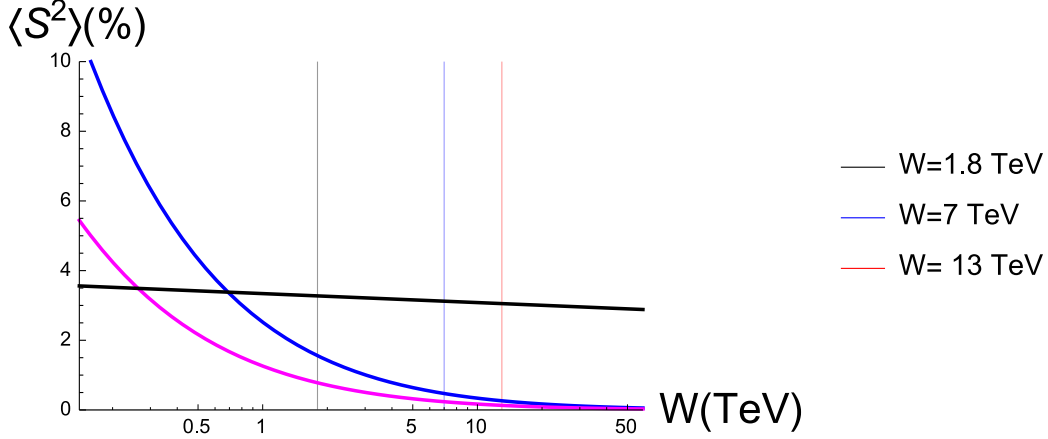


Figure 12. $\langle S^2 \rangle$ versus W . $\langle S^2 \rangle$ is calculated using Eq. (3.32) and Eq. (3.33) with Y replaced by $Y - \Delta_{cor} N_{G_{3P}}$ with $\Delta_{cor} = 2$ (blue curve), while the red curve is the same as in Fig. 9. The black curve is the estimates for the survival probability with new set of parameters (see Table 1).

4.4 Comparison with other estimates

Nearly ten years ago we summarized the situation regarding the evaluation of the $\langle S^2 \rangle$ by different models [37]. Unfortunately, as the results of this paper illustrate, the values obtained for $\langle S^2 \rangle$, are highly dependent on the characteristics of the models used to parametrize the soft and hard amplitudes. For details of the parametrizations used by the three groups quoted in Table 2, we refer the reader to [37–39]. Their values for the $\langle S^2 \rangle$ are given in Table 2.

In the summary of our previous approach for constructing a model based on $N=4$ SYM for strong coupling, and matching with the perturbative QCD approach [40], we discuss the results for $\langle S^2 \rangle$ obtained from this approach. We compared our results with those obtained by the Durham group [41]. The Durham

W (GeV)	KKMR (CD) [38]	Pythia [39]	GLM [37]
540	6.	n/a	6.6
1800	4.5	4.0	5.5
14000	2.	2.6	3.6

Table 2. Values of $\langle S^2 \rangle$ at different energies from the three different groups [37–39]. The results are given as percentages.

W (GeV)	This model(I)	This model(II)	This model(IIIn)	This model(III)	KMR [41]	GLM [40]
1800	7.6	0.86	3.34	1.68	2.8	7.02
7000	3.63	0.3	3.1	0.63	1.5	2.98
14000	2.3	0.25	3.05	0.44	1.	1.75

Table 3. Values of $\langle S^2 \rangle$ at different energies from the different groups [41] and [40] and from this model: I - the hard amplitude is given by Eq. (3.5) with $B = 4.5 \text{ GeV}^{-2}$ (see Fig. 10 and Fig. 11), II- the hard amplitude is given by Eq. (3.6) with old set of parameters; IIIn- is the same as II but with the new set of parameters; and III- is the same as II but the kinematic corrections are include. The $\langle S^2 \rangle$ results are in percentages.

model is a two-channel eikonal model where the Pomeron coupling to the diffractive eigenstates are energy dependent. They presented four different versions, in Table 3, we quote their results for model 4, their "favoured version".

As can be seen from Table 3, our results for $\langle S^2 \rangle$ obtained from the $N=4$ SYM approach are slightly larger than those given by the KMR approach, and larger than the results of our present model. The reasons for this have been discussed in subsection 4.2.

Comparing the results of different calculations given in Tables 2 and 3 with our present calculation, we see that the estimates using the same b -dependence of the hard amplitude $A_{\text{hard}} \propto \exp(-b^2/4B)$ (see Table 3 ‘this model(I)’), leads to results that are similar to the estimates obtained by the other groups. The b -dependence of the hard amplitude that follows from our present approach, produces small values for the survival probabilities with the old set of parameters, and reasonable values with the new set of parameters. We wish to emphasize that our b -dependence of our present model, has two advantages: it leads to the correct Froissart limit at large b , $A_{\text{hard}} \propto \exp(-\mu b)$; and at large momentum transfer (Q_T) it decreases as a power of Q_T , as one expects in perturbative QCD.

We wish to emphasize, that we made a second (new) fit to the experimental data, and obtained a new set of parameters, which leads to an increase in the values of the survival probabilities as shown in Table 3.

5 Conclusions

In this paper we calculated the survival probability for central diffractive production, and found at LHC energies, that its value is small. The small value obtained does not stem from the sum of enhanced diagrams, as in our previous models[42], but is due to the impact parameter dependence of the hard amplitude.

W (TeV)	σ_{tot} (mb)	σ_{el} (mb) (mb)	B_{el} (GeV^{-2})	single σ_{sd}^{LM} (mb)	diffraction σ_{sd}^{HM} (mb)	double σ_{dd}^{LM} (mb)	diffraction σ_{dd}^{HM} (mb)
0.576	61.4(62.3)	13 (12.9)	15.2 (15.2)	4.1(5.64)	1.42 (1.85)	0.3 (0.7)	0.22 (0.46)
0.9	68.2(69.2)	15.1 (15)	16 (16)	4.45 (6.25)	1.89 (2.39)	0.3 (0.77)	0.32 (0.67)
1.8	78.2(79.2)	18.3 (18.2)	17.1(17.1)	4.87 (7.1)	2.79 (3.35)	0.28 (0.89)	0.55 (1.17)
2.74	82.3(85.5)	19.7 (20.2)	17.63 (17.8)	5 (7.6)	3.49 (4.07)	0.27 (0.97)	0.74 (1.62)
7	99.9 (99.8)	25.6 (25)	19.6 (19.5)	5.38 (8.7)	5.66 (6.2)	0.2(1.15)	1.46 (3.27)
8	102.1 (101.8)	26.4 (25.7)	19.8 (19.7)	5.41 (8.82)	6.03 (6.55)	0.2 (1.17)	1.68 (3.63)
13	110.6(109.3)	29.5 (28.3)	20.8 (20.6)	5.47 (9.36)	7.67 (8.08)	0.17(1.27)	2.28 (5.11)
14	111.9 (110.5)	29.9 (28.7)	20.9 (20.7)	5.47 (9.44)	7.87 (8.34)	0.17(1.27)	2.32 (5.4)
57	137.8(131.7)	39.7 (36.2)	23.6 (23.1)	5.37 (10.85)	14.99(15.02)	0.11(1.56)	5.86 (13.7)

Table 4. The values of cross sections versus energy. σ_{sd}^{LM} and σ_{dd}^{LM} denote the cross sections for diffraction dissociation in the low mass region, for single and double diffraction, which stem from the Good-Walker mechanism. While σ_{sd}^{HM} and σ_{dd}^{HM} are used for diffraction in high mass, coming from the dressed Pomeron contributions.

The distinguishing feature of our model based on CGC/saturation approach, is that we use a framework where soft and hard processes are treated on the same footing. Hence, there is no need to introduce a special hard amplitude, as has been done in all previous attempts, to estimate the survival probability. It should be stressed that the main source for our small values of $\langle S^2 \rangle$, is the impact parameter dependence of the hard amplitude, for which we do not have any theoretical estimate. This is usually assumed to have a Gaussian form $A_{\text{hard}} \propto \exp(-b^2/(2B))$. The value of B was taken from the experimental data on the deep inelastic diffractive production of vector mesons. We demonstrated in this paper, that in spite of the fact, that our hard amplitude leads to experimental values of B , at small t , it yields a different behaviour than the Gaussian input, leading to small values of $\langle S^2 \rangle$ at high energies. We note, that the impact parameter dependence of our hard amplitude satisfies two theoretical features that are violated in the Gaussian b -dependence: at large b , $A_{\text{hard}} \propto \exp(-\mu b)$, and at large Q_T it decreases as a power of Q_T , as required by perturbative QCD.

We wish to stress that the values obtained for the survival probability depend mostly on the b -dependence of the hard amplitude. The most interesting result is that we can describe on the same footing both the soft and the hard amplitude. At first sight, the small values of $\langle S^2 \rangle$ contradict this the most basic idea of our approach. To show that this is not an inherent problem of our approach, we made a new fit to the all available soft data to show that we can obtain substantially larger values of the survival probability. It demonstrates that experimental measurements of this observable is a sensitive tool to determine the values of the phenomenological parameters of our model.

We present in this paper, the result of the first consistent approach to obtain both the soft and the hard amplitude from the same model. We hope that the data from the LHC on the survival probability, will be instrumental in determining the impact parameter dependence of the scattering amplitude.

6 Acknowledgements

We thank our colleagues at Tel Aviv university and UTFSM for encouraging discussions. Our special thanks go to Carlos Cantreras , Alex Kovner and Misha Lublinsky for elucidating discussions on the subject of this paper. This research was supported by the BSF grant 2012124 and by the Fondecyt (Chile) grant 1140842.

References

- [1] M. G. Poghosyan, J. Phys. G **38**, 124044 (2011) [arXiv:1109.4510 [hep-ex]]. ALICE Collaboration, “*First proton–proton collisions at the LHC as observed with the ALICE detector: measurement of the charged particle pseudorapidity density at $\sqrt{s} = 900$ GeV,*” arXiv:0911.5430 [hep-ex].
- [2] G. Aad *et al.* [ATLAS Collaboration], Nature Commun. **2**, 463 (2011) [arXiv:1104.0326 [hep-ex]].
- [3] CMS Physics Analysis Summary: “Measurement of the inelastic pp cross section at $\sqrt{s} = 7$ TeV with the CMS detector”, 2011/08/27.
- [4] F. Ferro [TOTEM Collaboration], AIP Conf. Proc. **1350**, 172 (2011) ; G. Antchev *et al.* [TOTEM Collaboration], Europhys. Lett. **96**, 21002 (2011), **95**, 41001 (2011) [arXiv:1110.1385 [hep-ex]]; G. Antchev *et al.* [TOTEM Collaboration], Phys. Rev. Lett. **111** (2013) 26, 262001 [arXiv:1308.6722 [hep-ex]].
- [5] ALICE Collaboration, Eur. Phys. J. C **65** (2010) 111 [arXiv:0911.5430 [hep-ex]].
- [6] ATLAS Collaboration, arXiv:1003.3124 [hep-ex].
- [7] S. Chatrchyan *et al.* [CMS and TOTEM Collaborations], *proton Eur. Phys. J. C* **74**(2014)10, 3053[arXiv : 1405.0722[hep – ex]]; V. Khachatryan*etal.*[CMSCollaboration],*hadrons in* JHEP **1002** (2010) 041 [arXiv:1002.0621 [hep-ex]].
- [8] V. Khachatryan *et al.* [CMS Collaboration], JHEP **1101** (2011) 079 [arXiv:1011.5531 [hep-ex]].
- [9] G. Aad *et al.* [ATLAS Collaboration], JHEP **1207** (2012) 019 [arXiv:1203.3100 [hep-ex]].
- [10] E. Gotsman, E. Levin and U. Maor, Eur. Phys. J. C **75** (2015) 1, 18 [arXiv:1408.3811 [hep-ph]].
- [11] E. Gotsman, E. Levin and U. Maor, Eur. Phys. J. C **75** (2015) 5, 179 [arXiv:1502.05202 [hep-ph]].
- [12] E. Gotsman, E. Levin and U. Maor, Phys. Lett. B **746** (2015) 154 [arXiv:1503.04294 [hep-ph]].
- [13] E. Gotsman, E. Levin and U. Maor, Eur. Phys. J. C **75** (2015) 11, 518 [arXiv:1508.04236 [hep-ph]].
- [14] L. V. Gribov, E. M. Levin and M. G. Ryskin, Phys. Rep. **100** (1983) 1.
- [15] A. H. Mueller and J. Qiu, Nucl. Phys. **B268** (1986) 427.
- [16] L. McLerran and R. Venugopalan, Phys. Rev. **D49** (1994) 2233, 3352; **D50** (1994) 2225; **D53** (1996) 458; **D59** (1999) 09400.
- [17] I. Balitsky, [arXiv:hep-ph/9509348]; *Phys. Rev.* **D60**, 014020 (1999) [arXiv:hep-ph/9812311]
- [18] Y. V. Kovchegov, *Phys. Rev.* **D60**, 034008 (1999), [arXiv:hep-ph/9901281].
- [19] A. H. Mueller, Nucl. Phys. **B415** (1994) 373; **B437** (1995) 107.
- [20] J. Jalilian-Marian, A. Kovner, A. Leonidov and H. Weigert, *Phys. Rev.* **D59**, 014014 (1999), [arXiv:hep-ph/9706377]; *Nucl. Phys.* **B504**, 415 (1997), [arXiv:hep-ph/9701284]; J. Jalilian-Marian,

- A. Kovner and H. Weigert, *Phys. Rev.* **D59**, 014015 (1999), [arXiv:hep-ph/9709432]; A. Kovner, J. G. Milhano and H. Weigert, *Phys. Rev.* **D62**, 114005 (2000), [arXiv:hep-ph/0004014]; E. Iancu, A. Leonidov and L. D. McLerran, *Phys. Lett.* **B510**, 133 (2001); [arXiv:hep-ph/0102009]; *Nucl. Phys.* **A692**, 583 (2001), [arXiv:hep-ph/0011241]; E. Ferreira, E. Iancu, A. Leonidov and L. McLerran, *Nucl. Phys.* **A703**, 489 (2002), [arXiv:hep-ph/0109115]; H. Weigert, *Nucl. Phys.* **A703**, 823 (2002), [arXiv:hep-ph/0004044].
- [21] Yuri V Kovchegov and Eugene Levin, “ *Quantum Chromodynamics at High Energies*”, Cambridge Monographs on Particle Physics, Nuclear Physics and Cosmology, Cambridge University Press, 2012 .
- [22] M. L. Good and W. D. Walker, *Phys. Rev.* **120** (1960) 1857.
- [23] E. A. Kuraev, L. N. Lipatov, and F. S. Fadin, *Sov. Phys. JETP* **45**, 199 (1977); Ya. Ya. Balitsky and L. N. Lipatov, *Sov. J. Nucl. Phys.* **28**, 22 (1978).
- [24] L. N. Lipatov, *Phys. Rep.* **286** (1997) 131; *Sov. Phys. JETP* **63** (1986) 904 and references therein.
- [25] J. D. Bjorken, *Phys. Rev. D* **47** (1993) 101.
- [26] Y. L. Dokshitzer, V. A. Khoze and T. Sjostrand, *Phys. Lett. B* **274** (1992) 116.
- [27] E. Gotsman, E. M. Levin and U. Maor, *Phys. Lett. B* **309** (1993) 199 [hep-ph/9302248].
- [28] E. Levin, *JHEP* **1311** (2013) 039 [arXiv:1308.5052 [hep-ph]].
- [29] A. H. Mueller and B. Patel, *Nucl. Phys.* **B425** (1994) 471. A. H. Mueller and G. P. Salam, *Nucl. Phys.* **B475**, (1996) 293. [arXiv:hep-ph/9605302]. G. P. Salam, *Nucl. Phys.* **B461** (1996) 512; E. Iancu and A. H. Mueller, *Nucl. Phys.* **A730** (2004) 460 [arXiv:hep-ph/0308315]; 494 [arXiv:hep-ph/0309276].
- [30] L. A. Harland-Lang, V. A. Khoze and M. G. Ryskin, arXiv:1508.02718 [hep-ph]; L. A. Harland-Lang, V. A. Khoze, M. G. Ryskin and W. J. Stirling, *Int. J. Mod. Phys. A* **29** (2014) 1430031 [arXiv:1405.0018 [hep-ph]]; L. A. Harland-Lang, V. A. Khoze, M. G. Ryskin and W. J. Stirling, *Eur. Phys. J. C* **69** (2010) 179 [arXiv:1005.0695 [hep-ph]]; L. A. Harland-Lang, *Phys. Rev. D* **88**, 034029 (2013), 1306.6661; V. A. Khoze, A. D. Martin, and M. G. Ryskin, *Phys. Lett. B* **401**, 330 (1997), hep-ph/9701419; *Eur. Phys. J. C* **14**, 525 (2000), hep-ph/0002072; A. B. Kaidalov, V. A. Khoze, A. D. Martin, and M. G. Ryskin, *Eur. Phys. J. C* **23**, 311 (2002), hep-ph/0111078.
- [31] E. Gotsman, E. Levin and U. Maor, gaps,” *Phys. Lett. B* **438** (1998) 229 [hep-ph/9804404]; model,” *Phys. Rev. D* **60** (1999) 094011 [hep-ph/9902294].
- [32] P.D.B. Collins, “*An introduction to Regge theory and high energy physics*”, Cambridge University Press 1977.
- [33] S. Chekanov *et al.* [ZEUS Collaboration], *PMC Phys. A* **1** (2007) 6 [arXiv:0708.1478 [hep-ex]]. *Eur. Phys. J. C* **24** (2002) 345 [hep-ex/0201043].
- [34] A. Aktas *et al.* [H1 Collaboration], *Eur. Phys. J. C* **46** (2006) 585 [hep-ex/0510016].
- [35] E. Levin, J. Miller and A. Prygarin, *Nucl. Phys.* **A806** (2008) 245, [arXiv:0706.2944 [hep-ph]].
- [36] R. Aaij *et al.* [LHCb Collaboration], *J. Phys. G* **41** (2014) 055002 [arXiv:1401.3288 [hep-ex]].
- [37] E. Gotsman, E. Levin, U. Maor, E. Naftali and A. Prygarin, [arXiv:0511060 [hep-ph]].
- [38] A.B. Kaidalov, V.A. Khoze, A.D. Martin and M.G. Ryskin, *Eur. Phys. J. C* **21** (2001) 521.[hep-ph/0105145].
- [39] L. Lonnblad and M. Sjodahl, *JHEP* **05**, (2005) 038 [hep-ph/0412111].
- [40] E. Gotsman, E. Levin and U. Maor, *Int.J.Mod.Phys. A* **30**, (2015) 1542000.

- [41] V.A. Khoze, A.D. Martin and M.G. Ryskin, Eur. Phys. J. C **73** (2013) 2503.[arXiv:1306.2149 [hep-ph]].
- [42] E. Gotsman, E. Levin, U. Maor and J. S. Miller, Eur. Phys. J. C **57** (2008) 689 [arXiv:0805.2799 [hep-ph]].